Widely Tunable Quantum Phase Transition from Moore-Read to Composite Fermi Liquid in Bilayer Graphene

Zheng Zhu, D. N. Sheng, and Inti Sodemann

Phys. Rev. Lett. **124**, 097604 — Published 5 March 2020

DOI: 10.1103/PhysRevLett.124.097604

Widely Tunable Quantum Phase Transition from Moore-Read to Composite Fermi Liquid in Bilayer Graphene

Zheng Zhu,[1] D. N. Sheng,[2] and Inti Sodemann[3]

[1]*Department of Physics, Harvard University, Cambridge, MA, 02138, USA*
[2]*Department of Physics and Astronomy, California State University, Northridge, CA, 91330, USA*
[3]*Max-Planck Institute for the Physics of Complex Systems, D-01187 Dresden, Germany*

We develop a proposal to realise a widely tunable and clean quantum phase transition in bilayer graphene between two paradigmatic fractionalized phases of matter: the Moore-Read fractional quantum Hall state and the composite Fermi liquid metal. This transition can be realized at total fillings $\nu = \pm 3 + 1/2$ and the critical point can be controllably accessed by tuning either the interlayer electric bias or the perpendicular magnetic field values over a wide range of parameters. We study the transition numerically within a model that contains all leading single particle corrections to the band-structure of bilayer graphene and includes the fluctuations between the $n = 0$ and $n = 1$ cyclotron orbitals of its zeroth Landau level to delineate the most favorable region of parameters to experimentally access this unconventional critical point. We also find evidence for a new anisotropic gapless phase stabilized near the level crossing of $n = 0/1$ orbits.

Introduction. The advancements in the quality of graphene and the increased sophistication of techniques to probe it have positioned it as a rich platform to study the strongly correlated physics of the quantum Hall regime. Recent hallmarks of this progress include the observation of bubble phases in monolayer graphene [1], even denominator fractional quantum Hall states near a pseudo-spin transition in monolayer graphene [2], fractional Chern insulators in graphene-hexagonal boron nitride hetero-structures [2], even denominator fractional quantum Hall states in bilayer graphene [3–5], the observation of exciton condensation in double bilayer graphene [6, 7], and new sequences of interlayer correlated fractional quantum Hall states in double-layer graphene [8].

In this letter, we would like to offer a proposal to reap yet another fruit of this progress. We will show that bilayer graphene (BLG) is an ideal platform to realize a particularly clean quantum phase transition between two remarkable fractionalized phases of matter: the composite fermi liquid (CFL) metal [9] and the non-Abelian Moore-Read (MR) fractional quantum Hall state [10]. Our study builds upon previous numerical studies [4, 11–14] by incorporating our recently refined understanding of the Hamiltonian of the nearly eightfold degenerate zero Landau level of BLG [15]. There are two key ingredients that allow to controllably tune through this phase transition. One of them, first recognized in Ref. [11], is that the cyclotron orbital character of one of the Landau levels can be tuned continuously from mostly $n = 1$ character at small perpendicular magnetic fields into mostly $n = 0$ at high perpendicular fields. The second is the ability to enhance the splitting between $n = 0$ and $n = 1$ cyclotron orbits via the interlayer electric bias [16], whereby reducing the quantum fluctuations that make the MR state unexpectedly strong at zero interlayer bias in experiments [4, 5] in order to facilitate its quantum melting into the CFL state. The expected phase diagram is depicted in Fig. 1.

Theoretically the MR state can be understood as a $p + ip$ paired state of the CFL [17, 18]. Unlike ordinary metals, the CFL has been argued to not have generic pairing instabilities at low temperatures [19, 20], although an earlier study

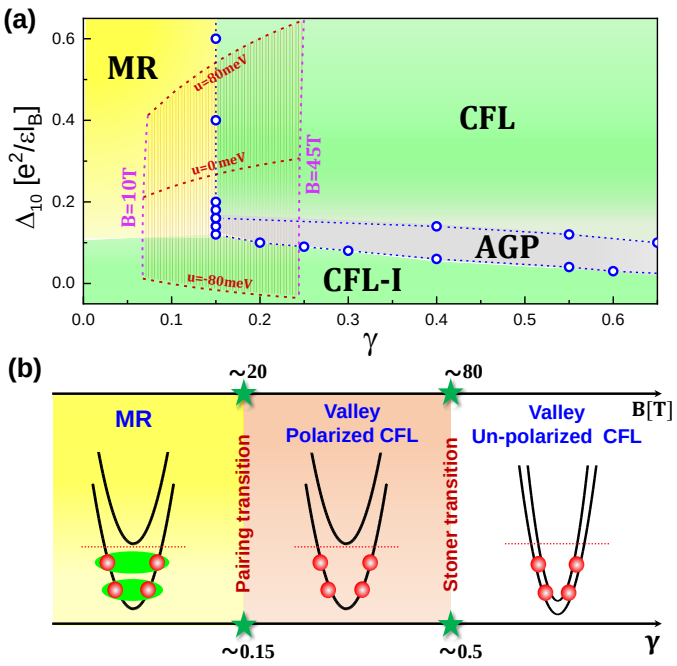

Fig. 1: (Color online) (a) Phase diagram of two-orbital model. Δ_{10} is the orbital splitting and γ parametrizes form factors controlled by magnetic field. We identify the MR, two types of CFL states, and an intermediate anisotropic gapless phase (AGP). The shaded region is the expected range of parameters accessed in BLG by tuning $B[T]$ and the interlayer electric bias u. (b) The phase diagram of SU(2) two-valley model [see Eq. 1] as a function of $B[T]$ or γ expected to be realised at $u = 0$. There are three phases: the valley polarized MR, and the valley polarized and un-polarized CFL states.

claimed the contrary [17]. If the CFL is stable against pairing, it would be possible to have an ideal stable phase transition from it into MR state by adding sufficiently large perturbations to the Hamiltonian. Originally, it was argued that this transition would be first order [19], but this conclusion was challenged more recently by studies that argued that a stable

continuous phase transition between the CFL and MR states is possible [20, 21]. Numerical studies support a possible continuous transition [22–24], although a definitive numerical conclusion is currently out of reach due to system size limitations, we have found certain features in the finite size spectra that indicate a possible continuous phase transition [34].

Experimentally, the phase transition has been studied by tuning subband level crossings [25, 26] and more recently hydrostatic pressure [27–29] in GaAs quantum wells. The subband level crossing, however, produces a rather abrupt change of the microscopic parameters of the Hamiltonian and the transition is therefore likely first order [24]. The isotropic hydrostatic pressure experiments, found the MR state transitions into a compressible phase with anisotropic transport properties, in resemblance to the transitions induced by applying in-plane field [30–33], and therefore potentially placing the problem on a different universality class from that of interest here. Additionally, one limitation of the pressure-driven platform is that it is difficult to capture it with an ideal Hamiltonian. Further details on these precedents are in [34].

Models and Key Results. The zero Landau level (ZLL) manifold of BLG comprises eight internal Landau levels that we denote by $\psi_{n,\tau,\sigma}$, where $n = \{0, 1\}$, $\tau = \{K, K'\}$ and $\sigma = \{\uparrow, \downarrow\}$ designates orbits, valleys and spins labels respectively. The ψ_1 orbitals can be approximated as having weight on the $n = 0$ and $n = 1$ cyclotron Galilean orbitals (denoted by $\phi_{0,1}$) [4, 13]: $\psi_{1,K} = (\sqrt{1-\gamma}\phi_1, 0, \sqrt{\gamma}\,\phi_0, 0)$ and $\psi_{1,K'} = (0, \sqrt{1-\gamma}\,\phi_1, 0, \sqrt{\gamma}\,\phi_0)$. Here, the different components denote amplitudes on (A, B', A', B) sites in Fig. 2 (b), and $\gamma \in [0, 1]$ is a parameter controlled primarily by the perpendicular magnetic field whose typical values are shown in Fig. 2 (c). On the other hand, the ψ_0 orbitals can be approximated as having only $n = 0$ Galilean orbitals: [4, 13] $\psi_{0,K} = (\phi_0, 0, 0, 0)$ and $\psi_{0,K'} = (0, \phi_0, 0, 0)$. A general interaction Hamiltonian projected onto a multi-flavor Landau level can be written as:

$$V = \sum_{\mathbf{q}\{\alpha\}} \frac{v(\mathbf{q})}{2A} F_{\alpha_1\alpha_2}(\mathbf{q}) F_{\alpha_3\alpha_4}(-\mathbf{q}) :\rho^{\dagger}_{\alpha_1\alpha_2}(\mathbf{q})\rho_{\alpha_3\alpha_4}(\mathbf{q}):, \quad (1)$$

where $v(\mathbf{q})$ is the Fourier transform of the un-projected interaction, $F_{\alpha\alpha'}(\mathbf{q})$ is the density form factor determined by the wavefunctions, and $\rho_{\alpha\alpha'}(\mathbf{q})$ are the flavor resolved intra-Landau-level guiding center density operators (see e.g. [35]). We set magnetic length $l_B \equiv \sqrt{\hbar c/eB}$ as the unit of length and $e^2/\varepsilon l_B$ as the unit of energy.

Our ideal Hamiltonian of interest is comprised of the Coulomb interaction projected onto the single $\psi_{1,\tau}$ Landau level. The form factor $F_{11}(\mathbf{q})$ is given by $F_{11}(\mathbf{q}) = (1-\gamma)F_1(\mathbf{q}) + \gamma F_0(\mathbf{q})$, where $F_{0,1}(\mathbf{q}) = \exp(-\mathbf{q}^2/4)L_{0,1}[\mathbf{q}^2/2]$ are the form factors for $n = 0$ and $n = 1$ Galilean Landau levels. Therefore the Hamiltonian continuously interpolates from a $n = 1$ Galilean Landau level at small γ (weak perpendicular fields) to an $n = 0$ Galilean Landau level at large γ (strong perpendicular fields). We have found that at half filling the MR is the ground state of this ideal Hamiltonian for $\gamma \lesssim 0.15$ whereas for $\gamma \gtrsim 0.15$ the CFL is the ground state. To demonstrate that this conclusion remains robust in the presence of other flavors and to delineate the region of parameters to realize such ideal limit within more realistic models, we will study several modifications to this ideal Hamiltonian.

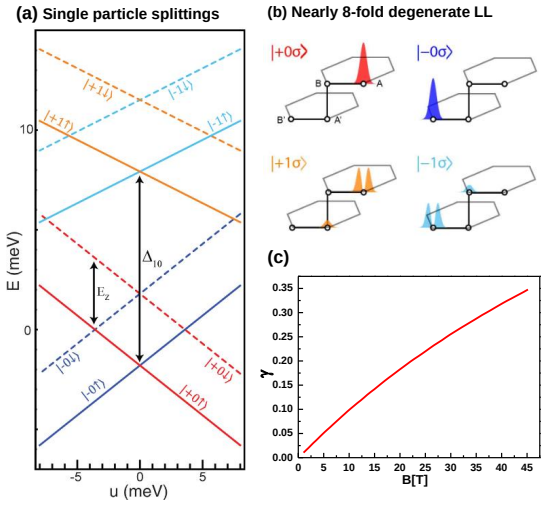

Fig. 2: (Color online) (a) The single particle splittings of BLG as a function of interlayer bias u. (b) The schematic depiction of the zero Landau level (ZLL) manifold of BLG $|\tau n\sigma\rangle$ on (A, B', A', B) sites. Here, $\tau = \{K, K'\} \equiv \{+, -\}$ denotes valleys, n and σ are LL and spin index, respectively. (c) The relationship between parameter γ and the magnetic field B. Figures (a) and (b) are from [15], the data of (c) is from [4].

The first modified Hamiltonian is an SU(2) symmetric version of the ideal Hamiltonian we just described, containing two-valleys $\psi_{1\alpha}$, $\alpha = \{K, K'\}$. Therefore the form factors are $F_{\alpha,\alpha'}(\mathbf{q}) = \delta_{\alpha,\alpha'}F_{11}(\mathbf{q})$. In this case we will show that the ground state spontaneously polarizes onto a single valley for $\gamma \lesssim 0.5$ and therefore the phase transition region from MR to CFL remains unmodified by the presence of a second degenerate valley (or spin). This interesting regime of vanishing single-particle valley splitting with spontaneous valley polarization can be best achieved at total filling $\nu = 3 + 1/2$ near zero interlayer bias $u \approx 0$. In the supplementary we describe how valley dependent interactions, which break the SU(2) valley symmetry down to U(1), are not expected to significantly affect the location of the phase transition.

The second modified Hamiltonian contains two Landau levels with different orbital character and the same valley $\psi_{\alpha K}$, $\alpha = \{0, 1\}$. There is no flavor conservation in this case and thus the form factors contain flavor off-diagonal components, and are given by: $F_{00}(\mathbf{q}) = F_0(\mathbf{q})$, $F_{11}(\mathbf{q}) = (1-\gamma)F_1(\mathbf{q}) + \gamma F_0(\mathbf{q})$, $F_{10}(\mathbf{q}) = [F_{01}(-\mathbf{q})]^* = \sqrt{1-\gamma}\exp(-\mathbf{q}^2/4)[-i(q_x + iq_y)/\sqrt{2}]$. We also add a single particle spliting Δ_{10} between these two orbital flavors. For this model, we will demonstrate that a single particle splitting, Δ_{10}, favouring $\psi_{1,K}$ over $\psi_{0,K}$ of about $\Delta_{10} \gtrsim 0.2e^2/\epsilon l_B$, is enough to reach the behavior of the ideal Hamiltonian con-

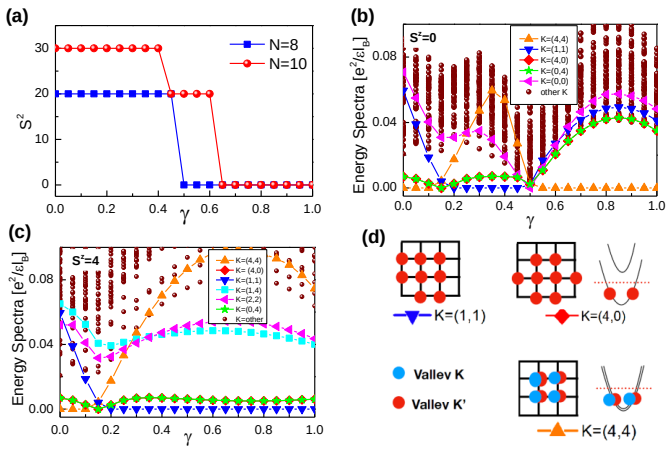

Fig. 3: (Color online) (a) The SU(2) Casimir operator S^2 as a function of γ. (b) and (c) show the energy spectra as a function of γ for valley-unpolarized sector (b) and valley-polarized sector (c). (d) The cluster of momentum determined by the trial wave function for polarized CFL (upper) and unpolarized CFL (lower).

taining only the $\psi_{1,K}$ Hamiltonian previously described. According to our estimates the built-in splitting between these orbitals in BLG is sufficient to reach this limit, but additionally, we will show that this splitting can be further enhanced at total filling $\nu = -3 + 1/2$ by applying interlayer effective field, giving us confidence that the ideal regime to realize the single-component MR to CFL transition can be accessed in BLG, in agreement with previous DMRG studies [4].

We will resort to numerical exact diagonalisation in the torus geometry [36, 37] to investigate the nature of the ground states as a function of γ and Δ_{10}. Throughout the main body of this paper we will focus on the Coulomb interaction, $v(\mathbf{q}) = 2\pi e^2/\epsilon|\mathbf{q}|$, however, in the supplementary we demonstrate that the key conclusions remain for more realistic interactions that account for screening [34].

Two-valley model. We begin by studying an SU(2) symmetric model including the ψ_{1K} and $\psi_{1K'}$ valleys. The ideal Hamiltonian describing a single valley can be obtained simply by restricting to the SU(2) subspace with maximal valley polarization. We denote the valley polarization as $S_z = (N_K - N_{K'})/2$. Figure 3 (a) depicts the value of SU(2) Casimir operator, S^2, which determines the valley polarization of the ground state as a function of γ. We find that the system jumps from a polarized state into a singlet at $\gamma \sim 0.5$, although a small intermediate range of γ with partial polarization cannot be completely discarded. It is well documented, experimentally [38–40] and numerically [41–43], that in the SU(2) limit the CFL in the $n = 0$ LL ($\gamma \to 1$) is a two-component unpolarized singlet. It is also well-established that in the SU(2) limit of an $n = 1$LL ($\gamma \to 0$) the MR state is a fully polarised ferromagnet spontaneously breaking the SU(2) symmetry [41, 44, 45]. The polarization we find is consistent with these expectations and it is therefore natural to conclude that in these limits we have a valley singlet CFL state at $\gamma \to 1$ and a valley polarized state at $\gamma \to 0$. However, we have found another phase at intermediate γ, namely, a single component Stoner-type CFL with spontaneous valley polarization.

We will now show that the quantum numbers of the states for $0.15 \lesssim \gamma \lesssim 0.5$ indeed are those of a fully polarized CFL while those of the state present for $\gamma \gtrsim 0.5$ correspond to a two-component un-polarized CFL. To do so, we consider trial CFL wavefunctions [46] in the torus [22, 36, 43, 47]. We review the construction of these trial CFL wavefunctions in [34]. The key quantum number that allows direct comparison with numerics is the many-body momentum, which, for the square torus reads as $\mathbf{K} = (L/N)\sum_i \mathbf{k}_i = (2\pi/N)\sum_i(-m_{2i}, m_{1i}) \mod(N)$ ($m_{1,2} \in Z \mod(N_\phi)$). This momentum in units of $(2\pi/N)$ is the same that labels the states of the spectrum in Fig. 3 (b) and (c) [48]. The cluster of momentum that correspond to the states that minimise the trial mean-field energy of a single component CFL [43] are $(K_x, K_y) \in (2\pi/N)\{(1,1),(4,0),(0,4)\}$ for $N = 8$ particles and are shown in Fig. 3 (d). We see that these states have the same quantum numbers of those obtained from exact diagonalisation for $0.15 \lesssim \gamma \lesssim 0.5$. Following a similar analysis for a two-component CFL singlet state [49], one can show that for 8 particles there is a unique finite size cluster forming a *closed shell* in momentum, namely, that the lattice of displacement vectors transforms trivially under the point group of the square torus. This state forms at momentum $(K_x, K_y) = (2\pi/N)(4,4) = (\pi,\pi)$ and is depicted in Fig. 3 (d). This is indeed coincides with the momentum of the ground state realized for $\gamma \gtrsim 0.5$ in Fig 3 (b) .

Therefore, we have found that the SU(2)-valley invariant system has three phases: (I) a valley polarized MR Pfaffian state for $\gamma \lesssim 0.15$, (II) a valley polarized single component CFL state for $0.15 \lesssim \gamma \lesssim 0.5$, and (III) a valley un-polarized two component CFL state for $\gamma \gtrsim 0.5$, as illustrated in Fig. 1 (b). For the ideal Hamiltonian from Eq. (1) of a single valley case then we would simply encounter phases (I) and (II). In the supplementary material [34] we demonstrate that these conclusions still hold for larger system sizes and for more realistic screened versions of the Coulomb interaction, and we also provide arguments for why the essential physics of the ground states under consideration are robust. For bilayer graphene, this leads us to expect that the transition between MR and CFL can be achieved near $\nu = \pm 3 + 1/2$ for $B \sim 20T$ [see Fig. 1 and Fig. 2(b)]. Unfortunately, the Stoner type transition between the single and two-component CFL states is expected at about $B \sim 80T$. A related Stoner transition between single and two component CFL states has been recently discussed in monolayer graphene [50].

Two-orbital model. A special feature of the zeroth Landau level of BLG is the relatively small energy splitting between the ψ_1 orbits with $n = 1$ cyclotron character and the ψ_0 orbits with $n = 0$ cyclotron character. Therefore it is important to assess how robust the phases are to quantum fluctuations between these levels. To do so, we consider a model with

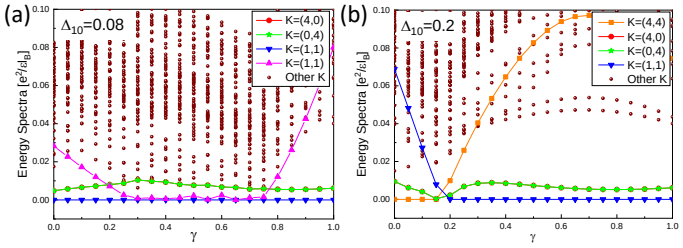

Fig. 4: (Color online)The energy spectra of two-orbital model as a function of γ at different single particle splitting Δ_{10} between ψ_0 and ψ_1 orbits: (a) $\Delta_{10} = 0.08$, (b) $\Delta_{10} = 0.2$.

the Coulomb interaction, $v(\mathbf{q}) = 2\pi e^2/\epsilon|\mathbf{q}|$, projected onto these two levels and an additional single particle splitting Δ_{10} favouring ψ_1. At total filling $\nu = 1/2$ it is clear that in the limit in which $\Delta_{10} \gg e^2/\epsilon l_B$, we will recover the physics of the ideal limit containing only the half-filled ψ_1 orbits.

The energy spectra of two-orbital model versus γ and Δ_{10} are shown in Figs. 4 and supplementary material [34]. We have found that this limit is achieved by a splitting $\Delta_{10} \gtrsim 0.2e^2/\epsilon l_B$ as shown in Fig. 1(a) and Fig. 4 (b). At smaller Δ_{10} we have found another CFL state labelled CFL-I in Fig. 1 (a). CFL-I is the ordinary CFL realized at half-filled ψ_0 orbit. The reason why this CFL becomes the ground state near $\Delta_{10} = 0$ is that there is an exchange energy gain to occupy $n = 0$ orbits due to the smaller spatial extension and hence larger exchange holes [35], and therefore at half-filling the state is the conventional $n = 0$ CFL. Here, Δ_{10} splits the degeneracy of the MR Pfaffian and anti-Pfaffian. An interesting possibility is that it could be possible, by controlling the interlayer bias, to tune experimentally from Pfaffian to anti-Pfaffian by changing the sign of Δ_{10}, as further discussed in [34].

Interestingly, we have also encountered an anisotropic gapless phase (AGP) at intermediate orbital splitting and magnetic field in Fig. 1(a). This phase features a multiplicity of low lying states and a robust ground state quasi-degeneracy indicative of a gapless broken symmetry state, as shown in Fig. 4 (a) and in the supplementary. Additionally the spectrum has a high sensitivity to changes of the aspect ratio of the torus, which indicates the breaking of rotational symmetry, shown in the supplementary [34]. This phase could be accessed in BLG near filling $\nu = 3 + 1/2$ and therefore we hope that future numerical and experimental studies can shed more light on its nature. We find that many phases meet near the $n = 1/0$ level crossing around $\Delta_{10} \sim 0.11e^2/\epsilon l_B$ and $\gamma \lesssim 0.15$ [34]. It is possible that other phases might be stabilized near this level crossing, such as the non-Abelian 221 parton state, as advocated in Ref. [51].We hope that future studies will further address this interesting possibility.

Region of parameters accessed in BLG. In Fig. 1(a) we have superimposed the expected range of parameters [52] that can be accessed in BLG by tuning perpendicular magnetic field and the interlayer electric bias u. The region for $u \leq 0$ should be accessible at $\nu = 3 + 1/2$, while the region of positive $u \geq 0$ should be accessible for $\nu = -3+1/2$. This can be inferred from Fig.2 which shows that the single particle level splitting Δ_{10} decreases with $|u|$ for $\nu = 3+1/2$ and increases with $|u|$ $\nu = -3 + 1/2$. Therefore, $\nu = -3 + 1/2$ can be brought much closer to the ideal limit to study the ideal CFL to MR transition by applying large interlayer bias, although different physics could be potentially accessed $\nu = 3+1/2$ with the interlayer bias, such as the nearly SU(2) valley symmetric conditions for $u \approx 0$ and the new intermediate anisotropic gapless phase (AGP) shown in Fig. 1(a).

Discussion and summary. We have advanced a proposal for realising a particularly clean and widely tuneable phase transition between the MR and CFL states in BLG at fillings $\nu = \pm 3 + 1/2$. The phase transition can be tuned by the perpendicular magnetic field, as in phase transitions previously realised in monolayer graphene [2, 14, 53, 54]. The simplest version of this phase transition is better achieved at $\nu = -3 + 1/2$ at large interlayer biases $|u| \gtrsim 50meV$, where we have demonstrated that both valley and orbital fluctuations become insignificant. This filling factor at such interlayer biases is therefore an ideal platform to study the CFL to MR transition. At the filling factor $\nu = 3+1/2$ one encounters increased valley fluctuations for vanishing interlayer bias, where one expects a near SU(2) valley symmetry. We have shown that this symmetry is spontaneously broken and the system is also expected to transition from a spontaneously valley polarised MR state into a spontaneously valley polarised Stoner CFL enriched by the physics of valley symmetry breaking. At this filling the interlayer electric field tends to enhance $n = 0/1$ orbital fluctuations, and this can be used to access a potentially new anisotropic gapless phase (AGP) near the level crossing of $n = 0$ and $n = 1$ orbits of a common valley as shown in Fig. 1(a).

We thank Liang Fu, T. Senthil, Jainendra Jain, Andrea Young and Ashvin Vishwanath for valuable discussions. This work was supported by the U.S. Department of Energy (DOE), Office of Basic Energy Sciences under Grant No. DEFG02-06ER46305. Z.Z. would like to gratefully acknowledge the computational resources at California State University Northridge for performing the numerical simulations.

[1] S. Chen, R. Ribeiro-Palau, K. Yang, K. Watanabe, T. Taniguchi, J. Hone, M. O. Goerbig, C. R. Dean, Phys. Rev. Lett. **122**, 026802 (2019).
[2] A. A. Zibrov, E. M. Spanton, H. Zhou, C. Kometter, T. Taniguchi, K. Watanabe and A. F. Young, Nature Physics **14**, 930 (2018).
[3] Ki, D.-K., Falko, V. I., Abanin, D. A. and Morpurgo, A. F.. Nano Letters **14**, 2135 (2014).
[4] Alexander A. Zibrov, Carlos. R. Kometter, Haoxin Zhou, Eric M. Spanton, Takashi Taniguchi, Kenji Watanabe, Michael P. Zaletel, Andrea F. Young, Nature **549**, 360 (2017).
[5] J. I. A. Li, C. Tan, S. Chen, Y. Zeng, T. Taniguchi, K. Watanabe, J. Hone, C. R. Dean, Science **358**, 648 (2017).
[6] Xiaomeng Liu, Kenji Watanabe, Takashi Taniguchi, Bertrand I.

Halperin, Philip Kim, Nature Physics **13**, 746(2017).
[7] J. I. A. Li, T. Taniguchi, K. Watanabe, J. Hone and C. R. Dean, Nature Physics **13**, 751 (2017).
[8] J.I.A. Li, Q. Shi, Y. Zeng, K. Watanabe, T. Taniguchi, J. Hone, C.R. Dean, Nature Physics (2019).
[9] B. I. Halperin, Patrick A. Lee, and Nicholas Read, Phys. Rev. B **47**, 7312 (1993).
[10] G. Moore, N. Read, Nucl. Phys. B **360**, 362 (1991).
[11] Vadim M. Apalkov and Tapash Chakraborty, PRL **107**, 186803 (2011).
[12] Z. Papić, D. A. Abanin, Y. Barlas, and R. N. Bhatt, Phys. Rev. B **84**, 241306(R) (2011).
[13] Z. Papić and D. A. Abanin, Phys. Rev. Lett. **112**, 046602 (2014).
[14] Z. Papić, R. Thomale, and D. A. Abanin, Phys. Rev. Lett. 107, 176602(2011).
[15] B. M. Hunt, J. I. A. Li, A. A. Zibrov, L. Wang, T. Taniguchi, K. Watanabe, J. Hone, C. R. Dean, M. Zaletel, R. C. Ashoori, A. F. Young, Nature Communications **8**, 948 (2017).
[16] T. Jolicoeur, C. Töke, and I. Sodemann, Phys. Rev. B **99**, 115139 (2019).
[17] M. Greiter, X. G.Wen, and F. Wilczek, Nucl. Phys. B **374**, 567 (1992).
[18] N. Read and D. Green, Phys. Rev. B **61**, 10267 (2000).
[19] N.E. Bonesteel, Phys. Rev. Lett. **82** 984 (1999).
[20] Max A. Metlitski, David F. Mross, Subir Sachdev, and T. Senthil, Phys. Rev. B **91**, 115111 (2015).
[21] Zhiqiang Wang, Ipsita Mandal, Suk Bum Chung, Sudip Chakravarty, Annals of Physics **351**,727 (2014) .
[22] E. H. Rezayi and F. D. M. Haldane, Phys. Rev. Lett. **84**, 4685 (2000).
[23] G. Möller, Arkadiusz Wójs, and Nigel R. Cooper, Phys. Rev. Lett. **107**, 036803 (2011).
[24] Z. Papić, F. D. M. Haldane, and E. H. Rezayi, Phys. Rev. Lett. **109**, 266806 (2012).
[25] Yang Liu, D. Kamburov, M. Shayegan, L. N. Pfeiffer, K. W. West, and K. W. Baldwin, Phys. Rev. Lett. **107**, 176805 (2011).
[26] J. Nuebler, B. Friess, V. Umansky, B. Rosenow, M. Heiblum, K. von Klitzing, and J. Smet, Phys. Rev. Lett. **108**, 046804 (2012).
[27] N. Samkharadze, K.A. Schreiber, G.C. Gardner, M.J. Manfra, E. Fradkin, G.A. Csáthy, Nat. Phys. 12, 191 (2016).
[28] K. A. Schreiber, N. Samkharadze, G. C. Gardner, Rudro R. Biswas, M. J. Manfra, and G. A. Csáthy, Phys. Rev. B **96**, 041107(R) (2017).
[29] K.A. Schreiber, N. Samkharadze, G.C. Gardner, Y. Lyanda-Geller, M.J. Manfra, L.N. Pfeiffer, K.W. West, G.A. Csáthy, Nature Nature Communications **9**, 2400 (2018).
[30] W. Pan, R. R. Du, H. L. Stormer, D. C. Tsui, L. N. Pfeiffer, K. W. Baldwin, and K. W. West, Phys. Rev. Lett. **83**, 820 (1999).
[31] M. P. Lilly, K. B. Cooper, J. P. Eisenstein, L. N. Pfeiffer, and K. W. West, Phys. Rev. Lett. **83**, 824 (1999)
[32] G. A. Csáthy, J. S. Xia, C. L. Vicente, E. D. Adams, N. S. Sullivan, H. L. Stormer, D. C. Tsui, L. N. Pfeiffer, and K. W. West, Phys. Rev. Lett. **94**, 146801 (2005).
[33] Zheng Zhu, Inti Sodemann, D. N. Sheng, Liang Fu, Phys. Rev. B **95**, 201116(R) (2017).
[34] see supplementary material for more details [55–73].
[35] G. F. Giuliani and G. Vignale, Quantum Theory of the Electron Liquid (Cambridge University Press, Cambridge,2005).
[36] F. D. M. Haldane, Phys. Rev. Lett. **55**, 2095 (1985).
[37] Daijiro Yoshioka, Phys. Rev. B **29**, 6833(1984).
[38] R. R. Du, A. S. Yeh, H. L. Stormer, D. C. Tsui, L. N. Pfeiffer, and K. W. West, Phys. Rev. Lett. **75**, 3926 (1995).
[39] I. V. Kukushkin, K. v. Klitzing, and K. Eberl, Phys. Rev. Lett. **82**, 3665 (1999).
[40] L. Tiemann, G. Gamez, N. Kumada, K. Muraki, Science **335**, 828 (2012).
[41] K. Park, V. Melik-Alaverdian, N. E. Bonesteel, and J. K. Jain, Phys. Rev. B 58, R10167(R) (1998).
[42] K. Park, J. K. Jain, Solid State Communications **119**, 291 (2001).
[43] Zheng Zhu, D. N. Sheng, Liang Fu, Inti Sodemann, Phys. Rev. B **98**, 155104 (2018).
[44] R. H. Morf, Phys. Rev. Lett. **80**, 1505 (1998).
[45] A. E. Feiguin, E. Rezayi, Kun Yang, C. Nayak, and S. Das Sarma,Phys. Rev. B **79**, 115322 (2009).
[46] E. Rezayi and N. Read, Phys. Rev. Lett. **72**, 900 (1994).
[47] N. Read, Semiconductor Science and Technology, **9**, 1859 (1994).
[48] We only show states in the upper quarter of the many-body Brillouin zone since the remainder are related by point group symmetry.
[49] More details on the construction of trial CFL states in the torus for two-component systems can be found in Ref. [43].
[50] Ajit C. Balram, Csaba Töke, A. Wójs, and J. K. Jain, Phys. Rev. B **92**, 205120 (2015).
[51] Ying-Hai Wu,Tao Shi,Jainendra K. Jain, Nano Lett. **17**, 4643 (2017).
[52] This region has been estimated using all the single-particle corrections (except for trigonal warping term) as described in Refs. [4, 15, 16]. We also included the Lamb-shift type vacuum correction to Δ_{10} [4, 15, 16]. We neglected screening corrections to the Coulomb interaction, taking simply $\epsilon \approx 6.6$ as relevant for hBN substrates. This omission can be taken as a worst case scenario estimate because screening will tend to reduce the scale of interactions relative to Δ_{10} pushing BLG effectively further into the large Δ_{10} limit. As described in the supplementary [34], we have explicitly verified that adding screening has no substantial effects on the MR to CFL transition in this limit.
[53] B. E. Feldman, B. Krauss, J. H. Smet, and A. Yacoby, Science **337**, 1196 (2012).
[54] B. E. Feldman, A. J. Levin, B. Krauss, D. A. Abanin, B. I. Halperin, J. H. Smet, and A. Yacoby, Phys. Rev. Lett.**111**, 076802 (2013).
[55] You, Y., Cho, G. Y. and Fradkin, E. Phys. Rev. B **93**, 205401 (2016).
[56] E. H. Rezayi, F. D. M. Haldane, and K. Yang, Phys. Rev. Lett. **83**, 1219 (1999).
[57] F. D. M. Haldane, E. H. Rezayi, and Kun Yang, Phys. Rev. Lett. **85**, 5396 (2000).
[58] Zheng Zhu, Inti Sodemann, D. N. Sheng, Liang Fu, Phys. Rev. B **95**, 201116(R) (2017).
[59] Y. Imry and S.-k. Ma, Phys. Rev. Lett. **35**, 1399 (1975).
[60] Y. Imry and M. Wortis, Phys. Rev. B **19**, 3580 (1979).
[61] M. Aizenman and J. Wehr, Phys. Rev. Lett. **62**, 2503 (1989).
[62] Maissam Barkeshli, Chetan Nayak, Zlatko Papić, Andrea Young, and Michael Zaletel, Phys. Rev. Lett. **121**, 026603 (2018).
[63] Michael P. Zaletel, Scott Geraedts, Zlatko Papić, and Edward H. Rezayi, Phys. Rev. B **98**, 045113 (2018).
[64] J. Falson, D. Tabrea, D. Zhang, I. Sodemann, Y. Kozuka, A. Tsukazaki, M. Kawasaki, K. von Klitzing, J. H. Smet, arXiv:1804.04565.
[65] Philipp Werner and Andrew J. Millis, Phys. Rev. Lett. **104**, 146401 (2010).
[66] E. V. Gorbar, V. P. Gusynin, V. A. Miransky, and I. A. Shovkovy,Phys. Rev. B 85, 235460 (2012).
[67] Kyrylo Snizhko, Vadim Cheianov, and Steven H. Simon, Phys.

Rev. B 85, 201415(R)(2012).
[68] M. Kharitonov, Phys. Rev. B **85**, 155439 (2012); M.Kharitonov, Phys. Rev. Lett. **109**, 046803 (2012).
[69] Inti Sodemann, Allan H. MacDonald, Phys. Rev. Lett. **112**, 126804 (2014).
[70] Fengcheng Wu, Inti Sodemann, Yasufumi Araki, Allan H. MacDonald, and Thierry Jolicoeur, Phys. Rev. B **90**, 235432 (2014).
[71] I. Sodemann, The fractional quantum Hall regime in graphene, PhD thesis, University of Texas at Austin, (2014).
[72] Edward H. Rezayi,Phys. Rev. Lett. 119, 026801 (2017).
[73] Thierry Jolicoeur, Csaba Tőke, and Inti Sodemann,Phys. Rev. B 99, 115139(2019).